



NOISE CHARACTERISTICS AND MEASUREMENT METHODOLOGY FOR TMR AND HALL-EFFECT CURRENT SENSORS

Cédric Simard, Systems Engineer
Allegro MicroSystems

INTRODUCTION

Many electrical and power systems, from electric vehicles to industrial automation, require accurate current-sensing measurements. While both Hall-effect and tunnel-magnetoresistance (TMR) current sensors provide excellent solutions for these measurements, optimal system performance requires careful consideration of distinct noise characteristics.

Hall-effect sensors have been the industry standard for decades. These sensors offer reliable performance with relatively constant noise characteristics across frequency. However, TMR technology introduces new possibilities for high-precision measurements. Most notably, TMR provides a noise profile of $1/f$, which dominates at low frequencies. In contrast, white noise characteristics dominate in Hall-effect sensors.

This application note provides a comprehensive guide to compare noise characteristics of TMR and Hall-effect current sensors. It explains measurement techniques, analysis methods, and practical design considerations to help engineers make informed decisions when selecting current sensors for specific applications.

NOISE FUNDAMENTALS

In magnetic sensors, noise originates from several fundamental sources. White noise is characterized by a constant power spectral density across all frequencies. Unlike frequency-dependent noise sources, white-noise spectral density, $S_v(f)$, remains constant. In frequency domain measurements, this results in a flat noise floor, expressed as:

Equation 1:

$$S_v(f) = K$$

where K is a technology-dependent constant.

Another significant noise source is $1/f$ noise (also called flicker noise). This noise component has a power spectral density that is inversely proportional to frequency:

Equation 2:

$$S_v(f) = K/f^\alpha,$$

where K is a technology-dependent constant, f is frequency, and α is typically close to 1. At low frequency, $1/f$ noise dominates; as frequency increases, $1/f$ noise rolls off and eventually becomes less significant than the white-noise floor.

The corner frequency is the frequency at which the white noise equals the flicker noise (see Figure 1).

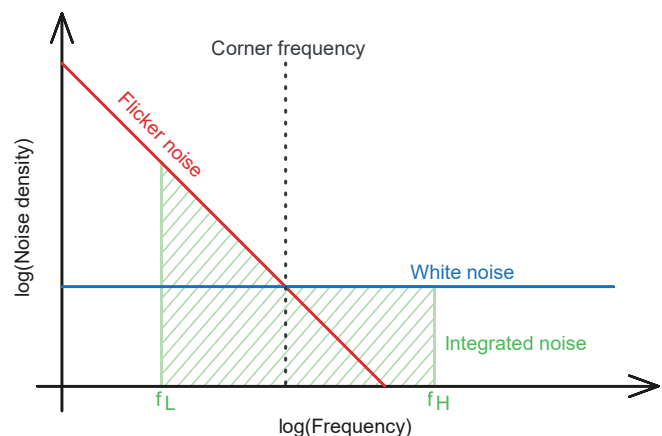


Figure 1: Noise density of flicker noise and white noise

To specify noise performance, two primary metrics are commonly used: Noise amplitude spectral density, $S_v(f)$, is expressed in $V/\sqrt{\text{Hz}}$ or $T/\sqrt{\text{Hz}}$ and represents the noise per unit bandwidth; and the integrated noise, obtained by integrating the noise power spectral density over the measurement bandwidth provides a complete picture of the sensor noise performance in the application, expressed as:

Equation 3:

$$V_{noise(RMS)} = \sqrt{\int_{f_L}^{f_H} S_v(f)^2 df}$$

where f_L and f_H define the measurement bandwidth of interest.

NOISE MEASUREMENT METHODOLOGY

Accurate noise characterization requires careful consideration of the measurement setup, equipment selection, and data acquisition parameters. The methodology presented here focuses on obtaining high-quality noise measurements across a wide frequency range, using an oscilloscope.

The measurement system consists of a device under test (TMR or Hall-effect sensor), a low-noise power supply using a lithium polymer (LiPo) battery and a low-dropout (LDO) regulator, a high-pass filter, a 34 dB low-noise amplifier (LNA), and a digital oscilloscope for data acquisition (see Figure 2). The

LiPo battery followed by the LDO regulator provides inherently low noise compared to switched-mode power supplies and eliminates powerline interference; this helps to minimize external noise sources and ensure measurement accuracy. The high-pass filter rejects the DC components of the sensor output, which would otherwise saturate the LNA.

The data acquisition uses a total of 20 million samples acquired over 20 seconds, resulting in a 1 MHz sampling rate. According to the Nyquist theorem, this allows spectral analysis at up to 500 kHz. The long acquisition time combined with a high sample count provides excellent frequency resolution at low frequencies and enables sufficient averaging at high frequencies.

The noise spectral density is computed using a variant of the Welch method for averaging modified periodograms. In the Welch technique, the time series is divided into overlapping segments, a window function is applied to each segment to reduce spectral leakage, and the discrete Fourier transform (DFT) of each windowed segment is computed, and their squared magnitudes are averaged. [1] The averaging process reduces the variance of the spectral estimate at the expense of frequency resolution. The variant used in this application note was developed to provide optimal frequency resolution for each Fourier frequency and more averaging at higher frequencies where the noise is typically more flat. [2]

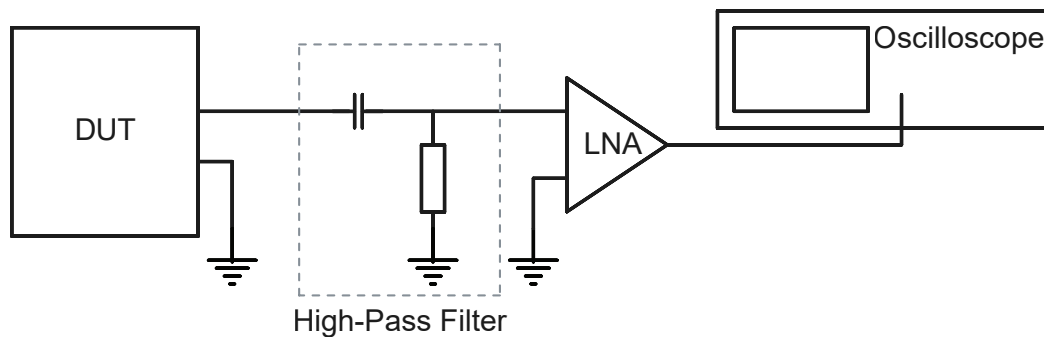


Figure 2: Measurement system

- [1] P. Welch, The use of fast Fourier transform for the estimation of power spectra: A method based on time averaging over short, modified periodograms, IEEE Transactions on Audio and Electroacoustics, vol. 15, no. 2, pp. 70–73, June 1967, doi: 10.1109/TAU.1967.1161901.
- [2] Michael Tröbs, Gerhard Heinzl, Improved spectrum estimation from digitized time series on a logarithmic frequency axis, Measurement, Volume 39, Issue 2, 2006, Pages 120–129, ISSN 0263-2241, doi: 10.1016/j.measurement.2005.10.010.

To establish measurement-system limitations and validate the setup, noise measurements were performed in three configurations: with inputs shorted to determine the system noise floor, on the power supply output voltage to verify the low-noise power source, and on the sensor output voltage for actual device characterization.

The measurement system capability was validated by characterizing three distinct noise spectral densities, as shown in Figure 3. To establish the intrinsic noise floor of the setup, shorted inputs were measured, providing a baseline reference (blue trace). The power supply noise demonstrates noise levels just above the measurement system floor. This result confirms the effectiveness of the LiPo battery and LDO regulator configuration. Finally, the sensor output (V_{OUT}) measurement clearly shows that the noise characteristics of the Allegro CT432-HSWF20MR XtremeSense TMR current sensor significantly exceed the system noise floor. This result validates the measurement methodology. This simple yet effective setup enables accurate noise characterization between 7 Hz and 500 kHz.

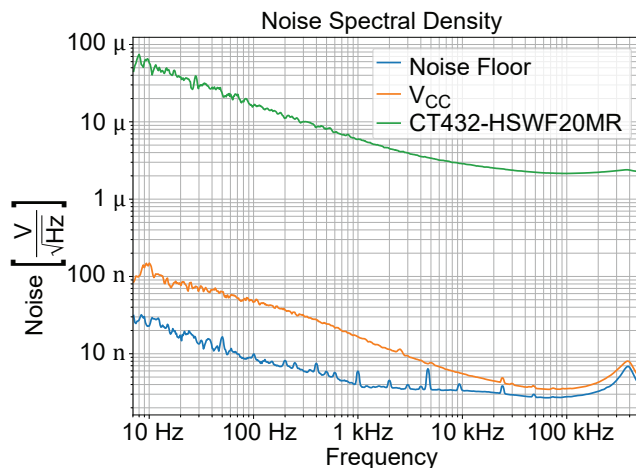


Figure 3: Noise spectral densities of the measurement setup, the power supply, and the output of the Allegro CT432 XtremeSense TMR current sensor

MAGNETIC SENSOR NOISE CHARACTERISTICS AND TECHNOLOGY COMPARISON

The noise performance of magnetic current sensors can be best understood through direct comparison of TMR and Hall-effect technologies. The noise spectral density measurements of three representative devices—two TMR sensors (CT4032-A20BSWF and CT432-HSWF20MR) and one Hall-effect sensor (ACS37010-30B5)—are shown in Figure 4. All measurements are expressed in input-referred units (A/\sqrt{Hz}) to enable direct comparison despite different sensor sensitivities. The current noise density is calculated by dividing the measured voltage noise density by the sensitivity of each sensor, expressed as:

Equation 4:

$$S_i(f) = \frac{S_v(f)}{\text{Sensitivity}}$$

where:

- $S_i(f)$ is the current noise density in A/\sqrt{Hz}
- $S_v(f)$ is the measured voltage noise density in V/\sqrt{Hz}
- Sensitivity is the sensor transfer function in V/A

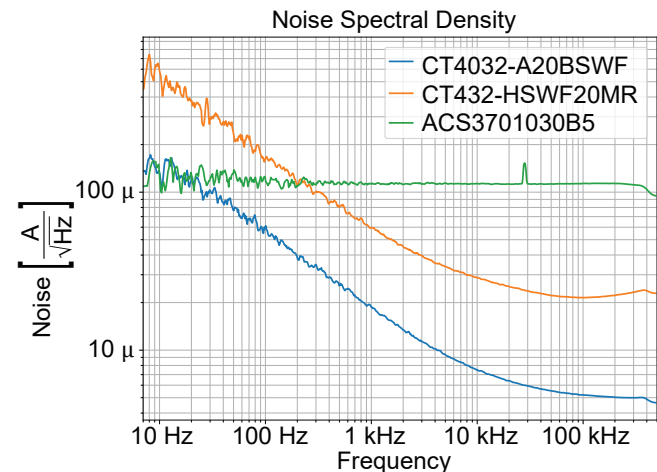


Figure 4: Noise spectral densities of different Allegro current sensors

TMR sensors exhibit characteristic $1/f$ noise behavior at low frequencies and transition to white noise at higher frequencies. The transition point, or corner frequency, is between 50 kHz and 200 kHz.

In contrast, at approximately $110 \mu\text{A}/\sqrt{\text{Hz}}$, the Hall-effect sensor demonstrates predominantly white-noise behavior across the frequency spectrum. Because the output of a Hall element is a very small voltage, achievement of the desired sensitivity requires significant amplification. The thermal noise of the Hall-plate resistance is thus extremely amplified.

Allegro MicroSystems Hall-effect sensors use dynamic quadrature offset cancellation, commonly referred to as “chopping,” to reduce the DC offset error. [3] However, because the $1/f$ noise is close to DC, this method also reduces the $1/f$ noise. Chopping consists of switching the Hall-plate voltage between two configurations at a high frequency. The offset error and $1/f$ noise are thus incorporated into this high frequency. The resulting signal is then demodulated to remove the high-frequency component.

By summing the contribution of each frequency to the total noise, the total integrated noise from 7 Hz to 500 kHz provides a comprehensive metric that can be used to compare sensor performance in typical applications. The measured root mean square (rms) noise for each sensor is summarized in Table 1.

These measurements demonstrate the superior noise performance of TMR technology. The TMR sensor CT4032-A20BSWF (from the Allegro CT4032/CT4022 family) achieves > 15 times less integrated noise than the Hall-effect sensor; and 4 times better noise performance than the previous TMR sensor generation, as compared to the CT432-HSWF20MR from the Allegro CT41x/CT42x/CT43x family.

While the Hall-effect sensor shows higher integrated noise, its other specifications continue to make it an excellent choice for applications where ultimate resolution is not the primary consideration.

Noise characteristics observed in the frequency domain are reflected in the time-domain waveforms shown in Figure 5. The Hall-effect sensor (ACS37010-30B5) exhibits a relatively uniform noise-distribution characteristic of white noise, with peak-to-peak variations of approximately 40 mV. The CT4032-A20BSWF demonstrates the lowest peak-to-peak noise variation among all sensors, consistent with its superior

integrated noise performance. These time-domain measurements provide an intuitive visualization of the noise behavior and complement the spectral analysis in assessing sensor performance for specific applications.

Table 1: Comparison of Integrated Noise of Different Allegro Current Sensors

Sensor Model	Technology	Integrated Noise (mArms)	Integrated Noise (mVrms)
CT4032-A20BSWF	TMR	3.86	0.386
CT432-HSWF20MR	TMR	16.6	1.66
ACS37010-30B5	Hall	76.5	5.11

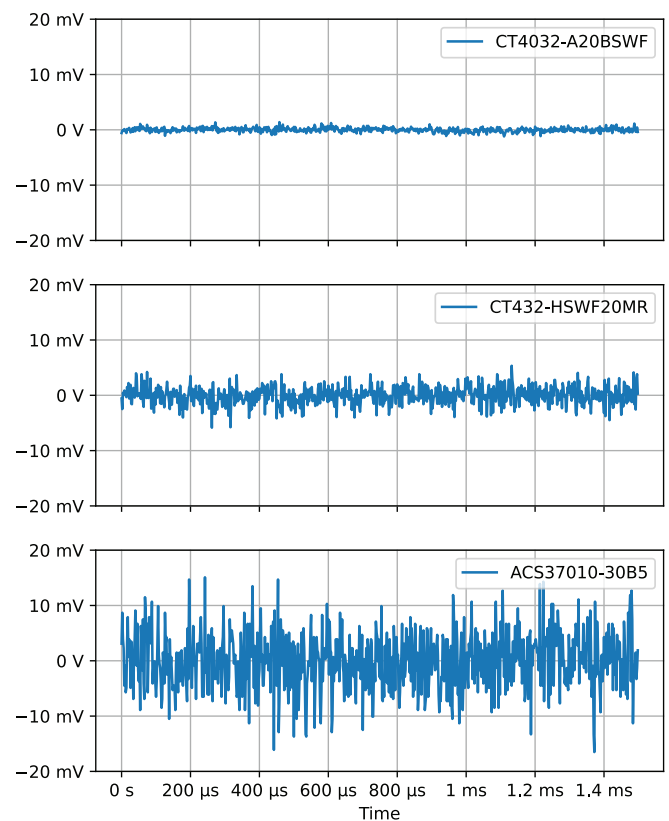


Figure 5: Noise waveforms in the time domain for different Allegro current sensors

[3] Alberto Bilotti, Life Senior Member, IEEE, Gerardo Monreal, and Ravi Vig, Monolithic Magnetic Hall Sensor ICs Using Dynamic Quadrature Offset Cancellation, <https://www.allegromicro.com/en/insights-and-innovations/technical-documents/hall-effect-sensor-ic-publications/monolithic-magnetic-hall-sensor-ics-using-dynamic-quadrature-offset-cancellation>

CONCLUSION

This analysis demonstrates distinct noise characteristics between TMR and Hall-effect current sensor technologies. The rigorous measurement methodology presented here demonstrates that, despite exhibiting characteristic $1/f$ noise at low frequencies, the CT4032-A20BSWF TMR sensor achieves up to 15 times less integrated noise than a traditional Hall-effect sensor. While Hall-effect sensors display more-consistent noise across frequency ranges, the best choice of technology ultimately depends on the specific application requirements. This comparative analysis provides engineers with quantitative data to make informed decisions for their current-sensing applications.

Revision History

Number	Date	Description	Responsibility
-	May 28, 2025	Initial release	C. Simard

Copyright 2025, Allegro MicroSystems.

The information contained in this document does not constitute any representation, warranty, assurance, guaranty, or inducement by Allegro to the customer with respect to the subject matter of this document. The information being provided does not guarantee that a process based on this information will be reliable, or that Allegro has explored all of the possible failure modes. It is the customer's responsibility to do sufficient qualification testing of the final product to ensure that it is reliable and meets all design requirements.

Copies of this document are considered uncontrolled documents.